

Determination of EM Coupling Effect in Dipole-Dipole Method : Complex Image Approach

Mester Sitepu

Universitas Sumatera Utara, Medan, Indonesia

Summary

Using the method of complex images, the electromagnetic coupling (Mutual Impedance) effect between the transmitter and the receiver that lie on the surface of a medium under investigation, is presented. Characteristics of electromagnetic coupling effect shows that the method of image is applicable in determining the electromagnetic coupling effect. For the horizontally homogeneous half-space medium and horizontally multilayer medium, the numerical results obtained are in highly agreement with those obtained using previously published methods. The electromagnetic coupling effect between the transmitter and the receiver and the apparent resistivity are also in agreement with the literature. Using the method of complex image, solution of the problem becomes simple and proven to be mathematically satisfactory to be used for determining the electromagnetic coupling effect in dipole dipole method.

Key words:

electromagnetic coupling, mutual impedance, complex image, apparent resistivity, reflection coefficient.

1. Introduction

Many solutions have been presented for solving the electromagnetic (EM) coupling problem. At the meeting in Tucson, Arizona, 1994, EM coupling (EMC) removal was still considered as the top priority for research in the IP method. The need for solving the EMC effect was stated clearly by Matthews and Zonge [1] by saying that the EMC and topography effects may contribute more than what we have known.

Image theory has been successfully applied in geophysical modeling. So far, the application of image theory, however, is limited to the problem of horizontally layered earth and/or uniformly dipping beds (i.e., Maeda [2] and Roman [3]). This image theory approach, known as the mirror image theory. This approach takes into account the multiple reflection effect. The resulting images of the multiple reflection effect become complicated for a complicated structure. The other image theory, known as the complex image theory, is the approach in which a multiple layer medium of finite conductivity is replaced by a perfectly conducting medium that is lying beneath the interface at a complex depth. The advantage of the complex image approach over the mirror image approach

alone is the existence of only one mirror (i.e., caused by the perfectly conducting medium). This is valid for both homogeneous and multilayer. Using the complex image approximation, therefore, should allow us to treat a multilayer medium as a homogeneous medium of characteristics ρ_1 and ρ_2 .

The general concept of mutual impedance (MI) and complex image approximation are presented. The MI based on the complex image approximation is derived, and the outcome for the dipole-dipole array are presented. For ready comparison with the results adopted by industries, the MI between the transmitter and the receiver (Tx and Rx) and the apparent resistivity of the medium under investigation are given.

2. Mathematical Approximation

In general, EMC is referred as the frequency dependence of the MI between two grounded wires: Tx and Rx. The EMC between Tx and Rx consists of wire to wire inductive coupling and the coupling through induction within the earth. The EMC generally considered as the imaginary part of the MI between Tx and Rx. The quantity of the MI between Tx and Rx is the same regardless of which circuit is the transmitter (Sunde [4]). Generally, the MI is defined as the ratio of the voltage (i.e., electromotive force) generated in the receiver to current introduced into the ground through the transmitter. Since the generated voltage is linearly proportional to the length of the receiver, the MI is also linearly proportional to the length of the receiver. Mathematically, the MI (Z_m) between Tx and Rx is:

$$Z_m = \frac{\int_M^N E_{//} dl}{I} \quad (1)$$

General view of the orientation of Tx and Rx, and the associated electric field components generated at the receiver are shown in Fig. 1. The total electric field generated by a transmitter of length AB can be obtained by integrating the whole length of transmitter. The MI between Tx and Rx, therefore, can be written as:

$$Z_m = \frac{1}{4\pi j\epsilon_0\omega} \iint_{MA}^{NB} \left(-\gamma_0^2 \Pi_x + \frac{\partial^2}{\partial x^2} \Pi_x + \frac{\partial^2}{\partial x \partial z} \Pi_z \right) ds dl$$

(2)

where $\gamma_0 = \mu_0 \epsilon_0 \omega^2$. Note that the constant

$$C = \frac{I ds}{4\pi j\epsilon_0\omega}$$

has been separated from the x and z components of the Hertz vector potential. Therefore, the x and z components of the Hertz vector potential appeared in Eq. 3 and Eq. 4 are those without C.

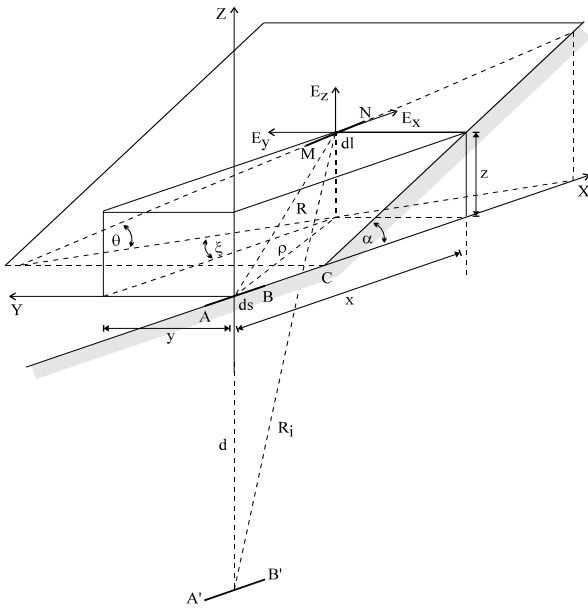


Fig. 1 General view of the transmitter AB and the receiver MN orientation. Note that the angle between the plane for Tx and Rx locations is $(180-\alpha)$. Note also that the origin of the Cartesian coordinate system is at the center of the transmitter AB, and A'B' is the image at a complex depth d from AB.

The modified components of the Hertz vector potential are (Sitepu and Susilawati [5]):

$$\Pi_x = \frac{e^{-\gamma_0 R_0}}{R_0} - \frac{e^{-\gamma_0 R_i}}{R_i} \tag{3}$$

$$\Pi_z = \frac{x}{\rho^2} \left(\frac{z e^{-\gamma_0 R_0}}{R_0} - \frac{(z+d) e^{-\gamma_0 R_i}}{R_i} \right) \tag{4}$$

From these, for the surface-to-surface propagation $\rho = x$,

$$R_0 = x \text{ and } R_i = \sqrt{x^2 + d^2} \text{ for the dipole-dipole array.}$$

If the MI between Tx and Rx is known, the commonly known parameters of the MI can be obtained. For a half space medium of infinite extent both laterally and

vertically downward, if the current introduced into the ground through the transmitter AB is I (see Fig. 2), the voltage detected by the receiver of length MN is generally written as:

$$V = \left(\frac{\rho_a I}{2\pi} \right) \left(\frac{1}{r_{BM}} - \frac{1}{r_{AM}} - \frac{1}{r_{BN}} + \frac{1}{r_{AN}} \right) \tag{5}$$

where ρ_a is the apparent resistivity of the medium under investigation, and r_{BM} , r_{AM} , r_{BN} and r_{AN} are distances between B and M, A and M, B and N and A and N respectively.

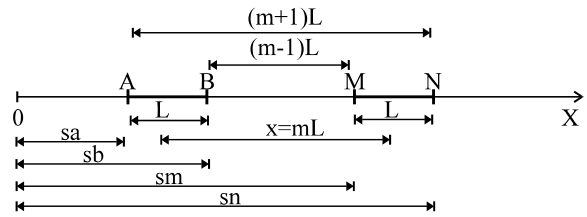


Fig. 2 Plan view of the system layout for the dipole-dipole array. Note that L is the dipole length, and $x=mL$ is the separation distance between Tx and Rx.

Rearranging the previous equation, the apparent resistivity of the half space medium can be written as:

$$\rho_a = 2\pi |Z_m| \left(\frac{r_{AN} r_{BN} (r_{AM} - r_{BM}) - r_{AM} r_{BM} (r_{AN} + r_{BN})}{r_{AM} r_{BM} r_{AN} r_{BN}} \right)$$

(6)

Note that $\frac{V}{I}$ has been replaced with the absolute value of

the MI between Tx and Rx (i.e., $|Z_m|$). Note also that since MI is the complex quantity, it is given in its absolute value. By referring to Fig. 2, for the dipole-dipole array we have $r_{AM}=mL$, $r_{AN}=(m+1)L$, $r_{BM}=(m-1)L$, $r_{BN}=mL$. Substituting these value into Eq. 6 and rearranging it, the apparent resistivity of the medium is:

$$\rho_a = |Z_m| \pi L m (m^2 - 1) \tag{7}$$

3. Results and Discussion

3.1. Characteristics Of Mutual Impedance

3.1.1. Traverse Distance Dependence

For the dipole-dipole array, measurements are normally conducted for moving both source and receiver. It is understood that, at a constant m distance and negligible ambient noise, measurements conducted over a homogeneous half space medium result in a constant MI.

To avoid the occurrence of constant MI, the MI is plotted as a function of m distance (i.e., fixed transmitter and

moving receiver).

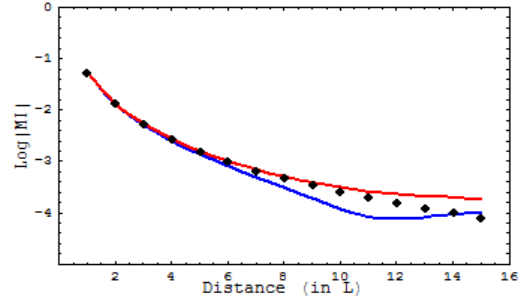
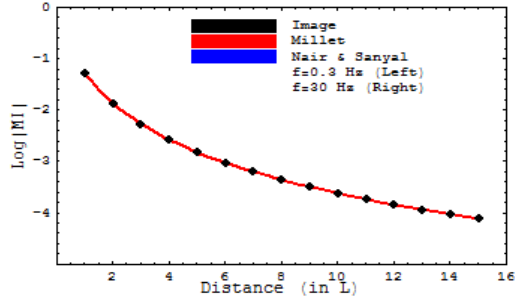


Fig. 3 Plots of MI as a function of distance for various frequency, at $\rho=100 \Omega\text{m}$ and $L=100$ meters

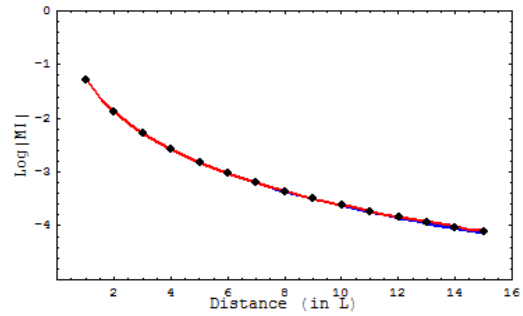
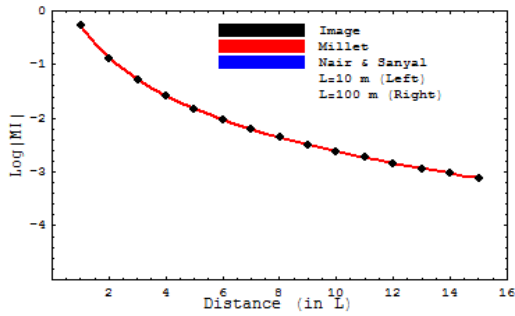


Fig. 4 Plots of MI as a function of distance for various conductivity, at $f=3 \text{ Hz}$ and $L=100$ meters.

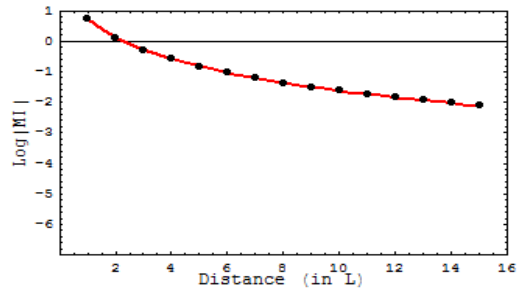
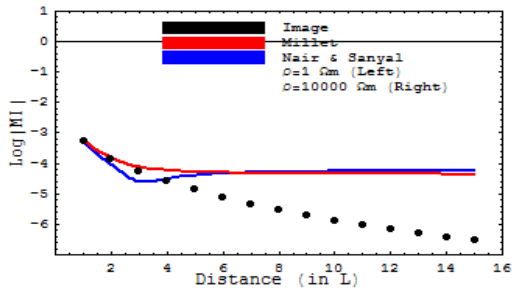


Fig. 5 Plots of MI as a function of distance for various dipole length, at $f=3 \text{ Hz}$ and $\rho=100 \Omega\text{m}$.

In order to be in the same magnitude as the results obtained by using the method derived by Nair and Sanyal [6] and those obtained by using the method given by Millet [7], the results obtained by using the method of images have to be calibrated with a factor of $1/\gamma_1$. This calibration factor is a part of the calibration factor used to

satisfy the boundary condition {i.e., γ_0^2/γ_1^2 (used by Bannister, [8] and Ward [9]) is equal to $1/\gamma_1 \gamma_0^2/\gamma_1$ and approximately the same as $1/\gamma_1 \gamma_0^2/\sqrt{f\sigma_1}$ }. Note that the x and z components of the electric field are obtained as

a result of double differentiation of the x and z components of the Hertz vector potential. Note also that the solution derived by Millet [7] and that given by Nair and Sanyal [6] are based on the equation given by Sunde [4], and these solutions are not exact.

3.1.2. Conductivity and Frequency Dependence

Let us take more extreme ranges of conductivity and frequency, but keep the variation of the dipole length at the common lengths used in the field. The selected range of conductivity is .00001 to 4 S/m, and that of frequency is 0.1 to 160 Hz. The selected dipole lengths are 10, 50 and 100 meters. Plots of MI as a function of conductivity and frequency are given in Fig. 6.

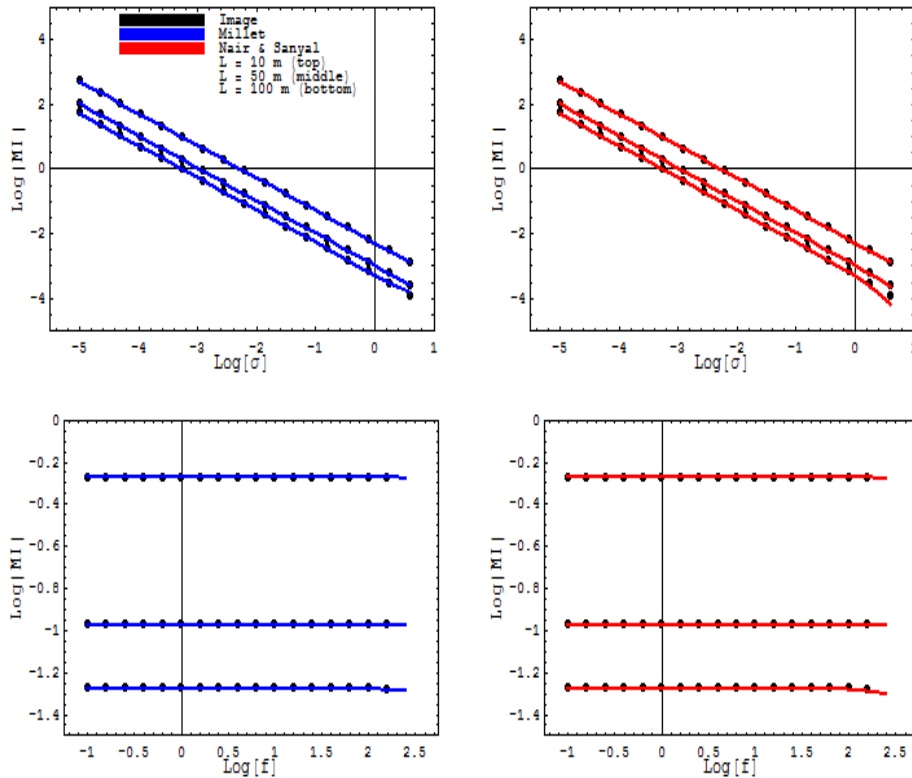


Fig. 6 Plots of MI as a function of conductivity and frequency for various dipole length.

3.2. Horizontally Homogeneous Half Space Medium

For ready comparison with the result obtained by using commercial software, the selected range of m distance is 2 to 7 (i.e., n ranges from 1 to 6), the common range of m distance in a pseudosection plot. In this case the selected dipole length is 100 meters. Plots of MI and apparent resistivity as a function of distance is given in Fig. 7.

3.3. Horizontally Multilayer Medium

The medium is assumed to consist of three homogeneous layers that extend infinitely laterally. Each layer has a constant thickness. The selected resistivity of the first layer is 100 m, the second layer is 10 m and the third layer is 300 m. The first layer is 100 meters thick, the second layer is 20 meters thick and the third layer is extending infinitely vertically downward. The selected lowest frequency is .3 Hz and the highest one is 3 Hz. The equations used to generate data are the same as those used in the homogeneous medium. To take into consideration the effect of multilayer medium, the depth of image is calculated by using Eq. 6, and 1 (i.e., following

Thomson and Weaver [10]) can be obtained recursively by using Eq. 7.

Prior to considering the multilayer medium the reliability of Eq. 6 and Eq. 7 are tested. The test is conducted by selecting the apparent resistivity of each layer is the same, 100 Ωm. In this case one would expect that the apparent resistivity obtained should be the same as that of homogeneous medium.

The same as in the homogeneous medium, the selected maximum m distance is 7. Note that m ranges from 2 to 7 in this method is equal to n ranges from 1 to 6 in the pseudosection plot. For $\rho_1 = \rho_2 = \rho_3 = 100 \text{ } \Omega\text{m}$, plot of apparent resistivity as a function of distance is given in Fig. 8. For different values of ρ_1 , ρ_2 and ρ_3 , plots of MI and apparent resistivity as a function of m distance are presented in Fig. 9.

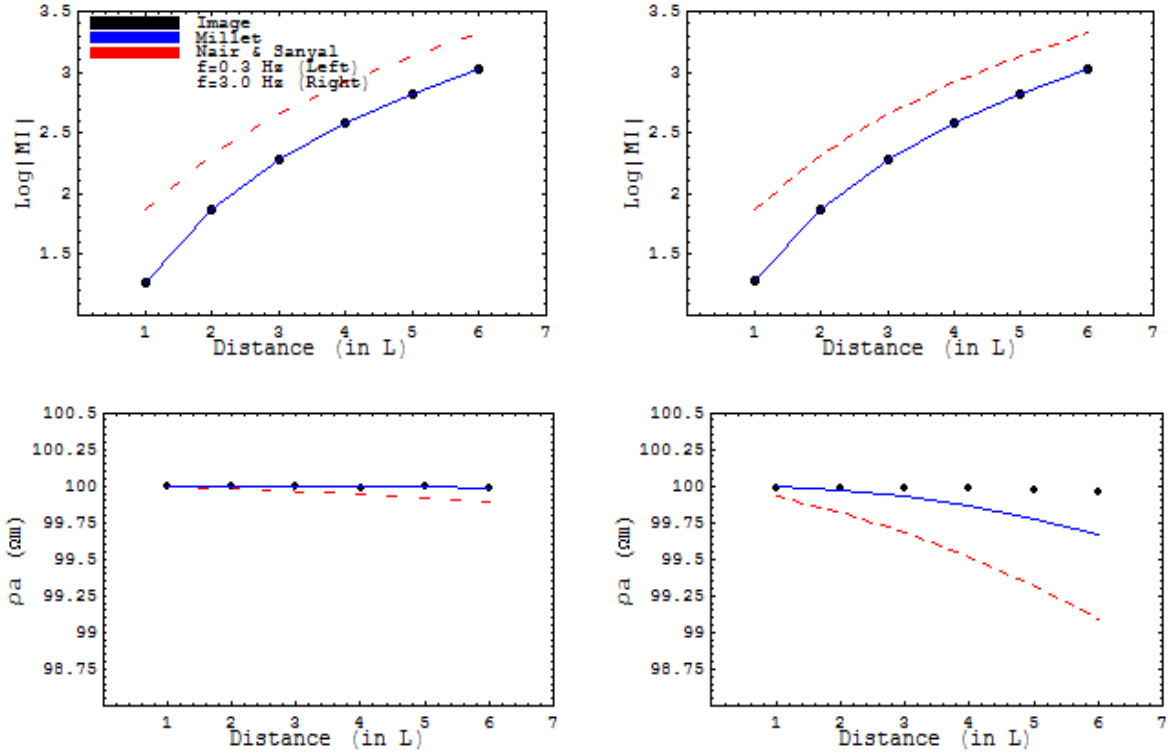


Fig. 7 Plots of MI and apparent resistivity as a function of distance for $\rho=100 \text{ } \Omega\text{m}$ and $L=100$ meters.

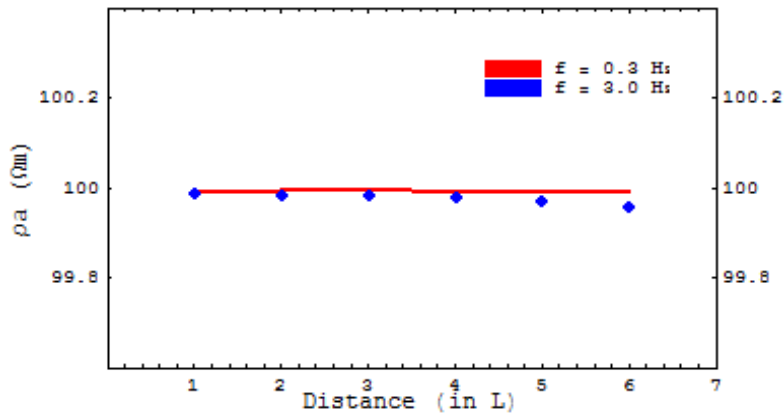


Fig. 8 Plots of apparent resistivity for a three layer medium of resistivities $\rho_1=100 \text{ } \Omega\text{m}$, $\rho_2=100 \text{ } \Omega\text{m}$, $\rho_3=100 \text{ } \Omega\text{m}$, $h_1=200$ meters and $h_2=50$ meters

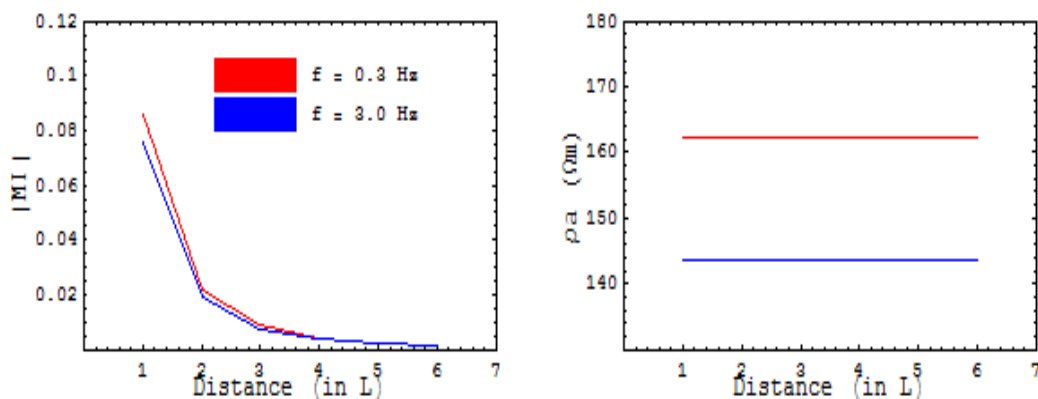


Fig. 9 Plots of Mutual Impedance and apparent resistivity as a function of m distance, for $L=100$ m, $\rho_1=100$ Ω m, $\rho_2=10$ Ω m, $\rho_3=300$ Ω m, $h_1=100$ meters and $h_2=20$ meters

From plots of MI as a function of frequency and that as a function of conductivity, for the selected parameters, the results obtained using the method given by Nair and Sanyal [6] and that derived by Millet [7] fit well those obtained using the method of images. These results show that within the generally used parameters in the field and commonly encountered conductivity of the overburden, the results obtained by using the method of images and those obtained by using the method given by Millet [7] and those obtained by using the method derived by Nair and Sanyal [6] are in highly agreement.

From plots of MI as a function of frequency and that as a function of conductivity we can conclude that the result obtained by using the method of images agrees with that obtained using the method given by Nair and Sanyal [6] and that obtained using the method derived by Millet [7]. These plots also suggest that within the generally used parameters in the field and commonly encountered conductivity of the overburden, the results obtained by using the method of images are satisfactory.

For observations over a horizontal half-space medium, using the dipole-dipole array, the MI obtained by applying the method of images fit well those obtained by using the method given by Millet [7] and those derived by Nair and Sanyal [6]. In agreement with our expectation, the effect of changing frequency from .3 Hz to 3 Hz is negligible. All methods agree with this result. Since the resistivity of the medium was selected as 100 Ω m, one would expect to get the apparent resistivity as 100 Ω m. However, due to the EMC effect the apparent resistivity decreases for increasing m distance and frequency. This means that the effect of EMC is better depicted by the plots of apparent resistivity. It is obvious that the method of images shows the least EMC effect, and on the other hand the method given by Nair and Sanyal [6] shows the highest EMC

effect. It is difficult to judge which method gives the most accurate result. The method derived by Millet [7] and that given by Nair and Sanyal [6] are derived from the equation given by Sunde [4]. Both methods show that the effects of frequency and conductivity are introduced by $\sqrt{\rho}$. Therefore, one would expect that the effects of EMC generated by these methods are the same. This is not the case. However, all methods show that, for the selected parameters, the effect of EMC is less than one percent.

From the observation over the homogeneous half-space medium we can conclude that the results obtained by using the method of images are in agreement with the results obtained by using the method given by Nair and Sanyal [6] and those obtained by using the method driven by Millet [7]. It is difficult to judge which method give the best result. However, all methods show that the EMC decreases the apparent resistivity value.

For observations over a multilayer medium, using dipole-dipole array, the first obvious result is that the change of MI and apparent resistivity as a result of changing frequency is obvious. It is also evident that the difference between the MI obtained at the highest frequency and that obtained at the lowest frequency is higher at shorter m distance. These were not the case in the homogeneous medium. To clarify this matter let us see the change that we have made in transforming the condition of a homogeneous medium to the condition of a multilayer medium. To take into account the effect of each layer, depth of image generated by a homogeneous medium was multiplied the factor of $\frac{1}{\rho}$. Since $\frac{1}{\rho}$ is frequency dependence (i.e., the value of $\frac{1}{\rho}$ is decreasing for increasing frequency) this result is not unexpected. An interesting result is that, although the difference between the MI obtained at the highest frequency and that obtained at the lowest frequency is decreasing for increasing m

distance, the difference between the apparent resistivity obtained at the highest frequency and that obtained at the lowest frequency is constant for increasing m distance. This indicates that, in terms of the change of apparent resistivity as a result of changing the EMC, the frequency is more dominant than the m distance. Evidently the apparent resistivity obtained at the lowest frequency is higher than that obtained at the highest frequency. This occurrence can be explained from the fact that a lower frequency penetrates deeper into the medium, thus the apparent resistivity detected is highly influenced by the lowest layer resistivity, and on the other hand a higher frequency results in a shallower penetration, thus the apparent resistivity obtained is less affected by the resistivity of the lowest layer. The result obtained, therefore, agrees with the expected result.

4. Conclusion and Suggestion

From plots of MI as a function of m distance we can conclude that using the method of images in calculating the MI between Tx and Rx is satisfactory. By comparing the result obtained by using the method of images and those obtained by using the method given by Millet [7] and those obtained by using the method driven by Nair and Sanyal [6], the method of images gives superior results.

Within the generally used parameters in the field and the commonly encountered conductivity of the overburden, the result obtained using the method of images is in highly agreement with that obtained using the method given by Millet [7] and that obtained using the method driven by Nair and Sanyal [6]. This suggests that the result obtained using the method of images is satisfactory. Failures of the method given by Millet [7] and that derived by Nair and Sanyal [6] in certain conditions show that the method of images is advantage. From these there is no doubt that the method of images can be used to calculate the MI between Tx and Rx.

Acknowledgments

Authors would like to acknowledge that part of the Research was Funded by the DGHE of Indonesia, under Hibah Bersaing Researc Grant. Support from USU is also greatly appreciated.

References

- [1] Matthews, P. and Zonge, K.L., "50 Years State of the Art in IP and Complex Resistivity." Proceeding of KEGS Anniversary Symposium Mining and Environmental Geophysics – Past, Present & Future, Toronto, Canada, , 2003.
- [2] Maeda, K., "Apparent Resistivity for Dipping Beds." Geophysics, vol . XX, no. 1 (1955), pp. 123-139.
- [3] Roman, I., "An Image Analysis of Multiple Layer Resistivity Problem." Geophysics, vol. XXIV, no. 3 (1959), pp. 485-509.
- [4] Sunde, E.D., Earth Conduction Effect in Transmission Systems, Dover Publication, New York, 1968.
- [5] Sitepu, M and Susilawati, "Solusi Vector Potensial Hertz Menggunakan Pendekatan Bayangan Komplek." Jurnal Penelitian MIPA (USU), vol. 2, no. 1 (2008), pp.8-16.
- [6] Nair, M.R. and Sanyal, N., "Electromagnetic Coupling in IP Measurements Using Some Common Electrode Arrays Over a Uniform Half-Space." Geopexploration, vol. 18 (1980), pp. 97-109.
- [7] Millet, F.B. Jr., Electromagnetic Coupling of Collinear Dipoles on a Uniform Half Space: in Mining Geophysics - Theory, vol. II, Society of Exploration Geophysics, Tulsa, Oklahoma, 1967, pp. 401-419.
- [8] Bannister, P.R., "Extension of Finitely Conducting Earth Image Theory Results to Any Range.", NUSC Technical Report 6885, 1984.
- [9] Ward, S.H., Part A: Electromagnetic Theory for Geophysical Applications, in Mining Geophysics - Theory, vol. II, Society of Exploration Geophysics, Tulsa, Oklahoma, 1967, pp. 10-196.
- [10] Thomson, D.J. and Weaver, J.T., "The Complex Image Approximation for Induction in a Multilayered Earth." Journal of Geophysical Research, vol. 80, no. 1 (1975), pp. 123-129.



Mester Sitepu received the B.S. and Drs. degrees in Physics from USU Medan Indonesia in 1978 and 1981, respectively. He then received the M.Sc. degree in Geophysical Engineering from CSM Golden USA in 1993. In 2009, he received his Doctorate degree from USU Medan Indonesia in Physico Chemistry. He has been working as a teaching fellow at USU since 1982. His research interest are in Computational Physics and Shallow Surface Geophysics.